



ELSEVIER

Theoretical and Applied Fracture Mechanics 34 (2000) 155–166

theoretical and
applied fracture
mechanics

www.elsevier.com/locate/tafmec

Microstructural effects on shear instability and shear band spacing

Li Chen, R.C. Batra *

Department of Engineering Science and Mechanics, MIC 0219, Virginia Polytechnic Institute and State University, Blacksburg, VA 24061, USA

Abstract

A constitutive relation that accounts for the thermally activated dislocation motion and microstructure interaction is used to study the stability of a homogeneous solution of equations governing the simple shearing deformations of a thermoviscoplastic body. An instability criterion and an upper bound for the growth rate of the infinitesimal deformations superimposed on the homogeneous solution are derived. By adopting Wright and Ockendon's postulate, i.e., the wavelength of the dominant instability mode with the maximum growth rate determines the minimum spacing between shear bands, the shear band spacing is computed. The effect of the initial dislocation density, the nominal strain-rate, and parameters describing the initial thermal activation and the initial microstructure interaction on the shear band spacing are delineated. © 2000 Elsevier Science Ltd. All rights reserved.

1. Introduction

Adiabatic shear bands are narrow regions of intense plastic deformation that usually form during high strain-rate deformation of several metals and some polymers. Their formation signals a transition from a generally homogeneous deformation to a nonhomogeneous one involving high strain gradients in a narrow region. These shear bands precede shear fractures. Thus there is significant interest in studying their initiation, propagation, width and spacing between adjacent bands.

The theoretical/analytical analyses of the problem can broadly be classified into two categories: (i) linear stability analysis, and (ii) numer-

ical solution of the coupled set of nonlinear equations. The linear stability analyses (e.g., see [1–7]) are aimed at delineating when a shear band initiates, and the spacing between them. The complete solution of the coupled nonlinear set of equations provides detailed information about the history of various deformation fields.

Most investigations have employed phenomenological constitutive relations. It was pointed out in [8–10] that these are valid only within the range of data used to calibrate them. These models do not account for the radically different behavior of face-centered-cubic (FCC) and body-centered-cubic (BCC) metals and the grain size. They [8–10] have proposed a constitutive relation that accounts for microstructural changes occurring in the body while it is being deformed. A dislocation mechanics based constitutive relation involving only one variable, namely, the total dislocation density has been proposed in [11–13]. This accounts for the effects of dislocation–dislocation

* Corresponding author. Tel.: +1-540-231-6051; fax: +1-540-231-4574.

E-mail address: rbatra@vt.edu (R.C. Batra).

interaction, evolution of subgrain size, grain diameter and twinning. Such a relation was used in [14] to study the initiation and development of shear bands in a layer with a small geometric defect and subjected to double shear impact loading. The primary characteristics of the computed solution are similar to those obtained with a phenomenological constitutive relation (e.g., see [15,16]).

A hybrid constitutive relation that accounts for the microstructural interaction [11–13] and thermally activated mechanisms [8–10] is used here. The linear stability analysis is performed to extend the instability condition [2] for a phenomenological constitutive relation to the present constitutive relation. The effect of microstructural parameters on the average strain when the homogeneous solution of the governing equations becomes unstable, and also on the minimum spacing between adjacent shear bands is delineated.

2. Formulation of the problem

Simple shearing deformations of an isotropic and homogeneous thermoviscoplastic body bounded by the planes $y = \pm h$ and sheared in the x -direction by prescribing velocities $v = \pm V_0$ on the upper and lower bounding surfaces are analyzed. The bounding surfaces are taken to be thermally insulated. Equations governing the deformations of the body are

$$\rho \ddot{\gamma} = \tau_{,yy}, \quad \dot{\gamma} = v_{,y}, \quad (1)$$

$$\rho c \dot{T} = k T_{,yy} + \beta \tau \dot{\gamma}, \quad (2)$$

$$\tau = \tau_1 + \tau_2, \quad (3)$$

$$\tau_1 = B_1 e^{-(\beta_1 - \beta_2 \ln \dot{\gamma})T} + B_2 \dot{\gamma}^{1/2} e^{-(\alpha_1 - \alpha_2 \ln \dot{\gamma})T}, \quad (4)$$

$$\tau_2 = b \alpha_0 \mu_0 (1 - AT - BT^2) \lambda^{1/2}, \quad (5)$$

$$\frac{d\lambda}{d\dot{\gamma}} = f(\lambda, \dot{\gamma}, T), \quad (6)$$

$$v|_{y=\pm h} = \pm V_0, \quad T_{,y}|_{y=\pm h} = 0. \quad (7)$$

Here ρ is the mass density, γ the shear strain, τ the shear stress, a superimposed dot denotes the ma-

terial time derivative, a comma followed by y the partial derivative with respect to y , c the specific heat, T the absolute temperature, k the thermal conductivity, and β is the Taylor–Quinney factor representing the fraction of plastic working converted into heating. Following the work in [8,12], τ is written as the sum of τ_1 and τ_2 . The part τ_1 of the shear stress given by (4) is contributed by the thermally activated dislocation interactions [8]. In it, B_1 , B_2 , β_1 , β_2 , α_1 and α_2 are constants; B_1 and B_2 are related to the reference Gibbs free energy, the dislocation activation area at zero temperature, and the magnitude of the Burger vector. For hexagonal closed-packed (HCP) metals, $B_1 \neq 0$, $B_2 \neq 0$; for face-centered-cubic (FCC) metals, $B_1 = 0$, $B_2 \neq 0$; and for body-centered-cubic (BCC) metals, $B_1 \neq 0$, $B_2 = 0$. The part τ_2 of the shear stress given by (5) depends on the thermo-mechanical history of the plastic deformation through the internal variable λ whose evolution is described by Eq. (6); this internal variable may be identified as the total dislocation density. In Eq. (5) b , α_0 , μ_0 , A and B are constants. The evolution rate, f , of λ is assumed to be nonnegative.

The stability of a homogeneous solution of the governing equations is studied herein; thus the initial conditions are not needed.

3. Instability analysis

The ordered set of variables γ, T, τ and λ is denoted by \mathbf{s} . In a time-dependent homogeneous solution of Eqs. (1)–(7), $v = V_0 y/h$. Such a solution is designated by $\tilde{\mathbf{s}} = (\tilde{\gamma}, \tilde{T}, \tilde{\tau}, \tilde{\lambda})^T$, and at time t_0 the infinitesimal perturbation

$$\delta \mathbf{s}(y, t, t_0) = e^{\eta(t-t_0)} e^{i\zeta y} \delta \mathbf{s}^0, \quad t \geq t_0, \quad (8)$$

is introduced. Here ζ is the wave number, η its growth rate at time t_0 . For the homogeneous solution to be unstable, $Re(\eta) > 0$; otherwise it is stable. Substitution of $\mathbf{s} = \tilde{\mathbf{s}} + \delta \mathbf{s}$ into Eqs. (1)–(7) and the linearization of the resulting equations in $\delta \mathbf{s}^0$ yield $\mathbf{A}(\mathbf{s}^0, \zeta, \eta, t_0) \delta \mathbf{s}^0 = \mathbf{0}$ which has a nontrivial solution only if $\det \mathbf{A} = 0$. This gives the following cubic equation for the growth rate η :

$$\begin{aligned} &\rho^2 c \eta^3 + \rho(-\beta \dot{\gamma}^0 \tau_{,T}^0 + k \xi^2 + c \tau_{,\dot{\gamma}}^0 \xi^2) \eta^2 \\ &+ (\beta \tau_{,T}^0 \tau_{,\xi}^2 + \rho c (f^0 \tau_{,\lambda}^0 + \tau_{,\dot{\gamma}}^0) \xi^2 + k \tau_{,\dot{\gamma}}^0 \xi^4) \eta \\ &+ k (f^0 \tau_{,\lambda}^0 + \tau_{,\dot{\gamma}}^0) \xi^4 = 0. \end{aligned} \tag{9}$$

Here $\tau_{,T}^0 = \partial \tau / \partial T|_{s=s^0}$, and the superscript zero on a variable signifies its value for the homogeneous solution at time t_0 . Variables $\tau_{,T}^0$, $\tau_{,\lambda}^0$, $\tau_{,\dot{\gamma}}^0$ and $\tau_{,\dot{\gamma}}^0$ denote, respectively, the thermal softening, hardening due to the increase in the dislocation density, strain-hardening and strain-rate hardening of the material. Note that $\tau_{,T}^0 \leq 0$, $\tau_{,\lambda}^0 \geq 0$, $\tau_{,\dot{\gamma}}^0 \geq 0$ and $\tau_{,\dot{\gamma}}^0 \geq 0$. Also, $f^0 \geq 0$, and ρ , c , k and β are positive. Thus the coefficients of η^3 , η^2 and the last term in Eq. (9) are positive. For Eq. (9) to have a positive root, it is necessary that $\tau_{,T}^0 < 0$. Hence, if $\tau_{,T}^0 = 0$, then there will be no instability implying thereby that thermal softening is a necessary condition for the onset of material instability.

In terms of nondimensional variables

$$\begin{aligned} \bar{\eta} &= \frac{k \eta}{c \tau_{,\dot{\gamma}}^0}, \quad \bar{\xi}^2 = \frac{k^2 \xi^2}{\rho c^2 \tau_{,\dot{\gamma}}^0}, \quad I = \frac{c \tau_{,\dot{\gamma}}^0}{k}, \\ J &= -\frac{\beta \tau_{,T}^0 \tau_{,\xi}^0 + \rho c f^0 \tau_{,\lambda}^0}{\rho c \tau_{,\dot{\gamma}}^0}, \quad C = -\frac{\beta k \tau_{,T}^0 \dot{\gamma}^0}{\rho c^2 \tau_{,\dot{\gamma}}^0}, \tag{10} \\ E &= 1 + \frac{f^0 \tau_{,\lambda}^0}{\tau_{,\dot{\gamma}}^0}, \end{aligned}$$

the spectral Eq. (9) becomes

$$\bar{\eta}^3 + [C + (1 + I) \bar{\xi}^2] \bar{\eta}^2 + [I \bar{\xi}^2 + 1 - J] \bar{\xi}^2 \bar{\eta} + E \bar{\xi}^4 = 0, \tag{11}$$

which is similar to Eq. (3.12) in [2]. For long wavelengths, $\bar{\xi} \rightarrow 0$ and three solutions of Eq. (11) are

$$\bar{\eta} = 0, \quad 0, \quad -C \tag{12}$$

which are all nonpositive. Thus, the homogeneous deformation is stable for perturbations with very long wavelengths. For extremely short wavelengths $\bar{\xi} \rightarrow \infty$. Dividing both sides of Eq. (11) by $\bar{\xi}^4$ and taking the limit as $\bar{\xi} \rightarrow \infty$, there results

$$\bar{\eta} = -k(\tau_{,\dot{\gamma}}^0 + f^0 \tau_{,\lambda}^0) / (\tau_{,\dot{\gamma}}^0 c \tau_{,\dot{\gamma}}^0) \leq 0 \tag{13}$$

and the shear deformation is again stable. Thus, if an instability occurs, it must occur at $0 < \bar{\xi} < \infty$.

For the given values of t_0 and $\bar{\xi}$, Eq. (11) will have either all three real roots or one real root and two complex conjugate roots; the root $\bar{\eta}_m$ with the largest positive real part will govern the instability of the homogeneous solution $\mathbf{s}^0 = \tilde{\mathbf{s}}(t_0)$. For fixed t_0 , $\bar{\eta}_m$ is a function of $\bar{\xi}$. Assume that $\bar{\eta}_m$ is real which is the case for perturbations introduced after the shear stress has attained its peak value. The wave number $\bar{\xi}_m$ for which $\bar{\eta}_m$ is maximum can be computed from

$$\frac{\partial \bar{\eta}}{\partial \bar{\xi}} \Big|_{(\bar{\eta}=\bar{\eta}_m, \bar{\xi}=\bar{\xi}_m)} = 0. \tag{14}$$

Eqs. (11) and (14) give

$$\bar{\xi}_m^2 = \bar{\eta}_m \frac{(J - 1) - (1 + I) \bar{\eta}_m}{2(E + I \bar{\eta}_m)}. \tag{15}$$

The requirement $\bar{\xi}_m^2 \geq 0$ implies that

$$0 \leq \bar{\eta}_m \leq \frac{(J - 1)}{(1 + I)} \equiv \eta_m^*. \tag{16}$$

Evaluating Eq. (11) at $(\bar{\xi}, \bar{\eta}) = (\bar{\xi}_m, \bar{\eta}_m)$, and substituting for $\bar{\xi}_m$ from (15) results in

$$\begin{aligned} 4(I \bar{\eta}_m + E)(\bar{\eta}_m + C) &= [(J - 1) - (1 + I) \bar{\eta}_m]^2 \\ &= (1 + I)^2 (\bar{\eta}_m - \eta_m^*)^2. \end{aligned} \tag{17}$$

Following the reasoning used in [2], it is concluded that whenever

$$J > 1 + 2\sqrt{EC}$$

or

$$\begin{aligned} &-\frac{\beta \tau_{,T}^0 \tau_{,\xi}^0}{\rho c \tau_{,\dot{\gamma}}^0} - \frac{f^0 \tau_{,\lambda}^0}{\tau_{,\dot{\gamma}}^0} \\ &> 1 + 2 \sqrt{-\left(1 + \frac{f^0 \tau_{,\lambda}^0}{\tau_{,\dot{\gamma}}^0}\right) \frac{\beta k \tau_{,T}^0 \dot{\gamma}^0}{\rho c^2 \tau_{,\dot{\gamma}}^0}}, \end{aligned} \tag{18}$$

Eq. (17) has a solution $\bar{\eta}_m > 0$. Thus Eq. (18) is the instability condition. If $f^0 = 0$ or $\tau_{,\lambda}^0 = 0$, then Eq. (18) reduces to Bai's criterion for instability, i.e. Eq. (4.1) in [2].

For locally adiabatic deformations, $k = 0$ and the instability criterion (18) becomes

$$-\frac{\beta\tau^0\tau_{\dot{\gamma}}^0}{\rho c\tau_{\dot{\gamma}}^0} - \frac{f^0\tau_{\lambda}^0}{\tau_{\dot{\gamma}}^0} > 1. \quad (19)$$

It follows from Eqs. (18) and (19) that the strain-rate hardening of the material does not directly influence the initiation of material instability. However, it affects the values of τ^0 , f^0 etc., and indirectly influences the onset of the material instability. Eq. (19) implies that for locally adiabatic deformations the material instability will occur only when the thermal softening exceeds the combined effects of the hardening of the material due to plastic straining and an increase in the dislocation density. However, in the presence of heat conduction, higher values of the nominal strain-rate delay the onset of material instability.

4. Numerical results and discussion

Numerical results are computed for a high strength steel with the function f in Eq. (6) taken as

$$\begin{aligned} f(\lambda, \dot{\gamma}, T) &= M - K_a(\dot{\gamma}, T)(\lambda - \lambda_0), \\ K_a(\dot{\gamma}, T) &= K_0, \quad 0 < T \leq T_a, \quad \text{or } \dot{\gamma} \geq \dot{\gamma}_0, \\ K_a(\dot{\gamma}, T) &= K_0(\dot{\gamma}/\dot{\gamma}_0)^{-2m_0}, \quad T \geq T_a, \quad \text{and } \dot{\gamma} \leq \dot{\gamma}_0, \end{aligned} \quad (20)$$

where M is the multiplication factor, K_a the annihilation factor, λ_0 the initial dislocation density, K_0 the annihilation constant at $T = 0$, m_0 the absolute strain-rate hardening sensitivity, and T_a is the transition temperature. The multiplication factor M is related to the mean free path of dislocations and the magnitude of the Burgers vector. M is taken to be a constant in this work. When $0 \leq T \leq T_a$ or $\dot{\gamma} \geq \dot{\gamma}_0$, Eq. (6) can be integrated with the following result:

$$\lambda = \lambda_0 + \frac{M}{K_a}(1 - e^{-K_a\gamma}). \quad (21)$$

A homogeneous solution of Eqs. (1)–(7) and Eq. (20) is

$$\tilde{\mathbf{s}} = \begin{Bmatrix} \tilde{\gamma} \\ \tilde{T} \\ \tilde{\tau} \\ \tilde{\lambda} \end{Bmatrix} = \begin{Bmatrix} \gamma_0 + \frac{V_0}{h}t \\ \tilde{T}(t) \\ \tilde{\tau}(\tilde{T}) \\ \lambda_0 + \frac{M}{K_a}(1 - e^{-K_a\tilde{\gamma}}) \end{Bmatrix} \quad (22)$$

where \tilde{T} is a solution of

$$\tilde{T}_{,T} = \frac{\beta\dot{\gamma}^0}{\rho c} \tilde{\tau}(\tilde{T}), \quad \tilde{\tau}(\tilde{T}) = \tau|_{(\gamma=\tilde{\gamma}, \dot{\gamma}=\dot{\gamma}^0, \lambda=\tilde{\lambda}, T=\tilde{T})}, \quad (23)$$

$\dot{\gamma}^0 = V_0/h$ is the prescribed nominal strain-rate and γ_0 is the initial strain.

The following values are assigned to various material parameters when computing numerical results:

$$\begin{aligned} B_1 &= 1.17 \text{ GPa}, \quad \beta_1 = 6.6 \times 10^{-3}/\text{K}, \\ \beta_2 &= 3.4 \times 10^{-4}/\text{K}, \quad K_0 = 9.23, \\ m_0 &= 1.47 \times 10^{-4}, \quad \beta = 0.9, \\ A &= 3.564 \times 10^{-6}/\text{K}, \quad B = 3.026 \times 10^{-7}/\text{K}^2, \\ b &= 2.48 \times 10^{-10} \text{ m}, \quad \lambda_0 = 6.2 \times 10^{12}/\text{m}^2, \\ M &= 1.2 \times 10^{14}/\text{m}^2, \quad \alpha_0 = 5.38, \\ \mu_0 &= 84 \text{ GPa}, \quad \rho = 7855 \text{ kg/m}^3, \\ k &= 60 \text{ W/(mK)}, \quad c = 460 \text{ J/(kg K)}, \\ T_0 &= 300 \text{ K}, \quad \gamma_0 = 0.01, \quad \dot{\gamma}_0 = 10^4/\text{s}, \\ T_a &= 558 \text{ K}. \end{aligned} \quad (24)$$

Here T_0 is the initial temperature and λ_0 is the initial dislocation density. Values in Eq. (24) for a high strength steel are chosen for illustrative purposes only, and are taken from [14]. When studying the effect of a material parameter on the localization process, all other material parameters were kept fixed.

Figs. 1(a)–(c) exhibit the evolution of the shear stress, the temperature and the dislocation density for homogeneous simple shearing deformations of the body at nominal strain-rates of 10^3 , 10^4 and $10^5/\text{s}$. It is clear that the shear stress required to plastically deform the material increases with an increase in the nominal strain-rate. For a fixed nominal strain-rate, the shear stress first increases because of the strain-hardening of the material, attains a maximum value at $\gamma \simeq 0.2$ when the softening of the material due to its being heated up equals its hardening, and subsequently decreases with an increase in the shear strain. The temperature increases monotonically because the boundaries of the body are thermally insulated and heat is generated due to plastic working. The temperature rise equals about 30 K when the peak in the

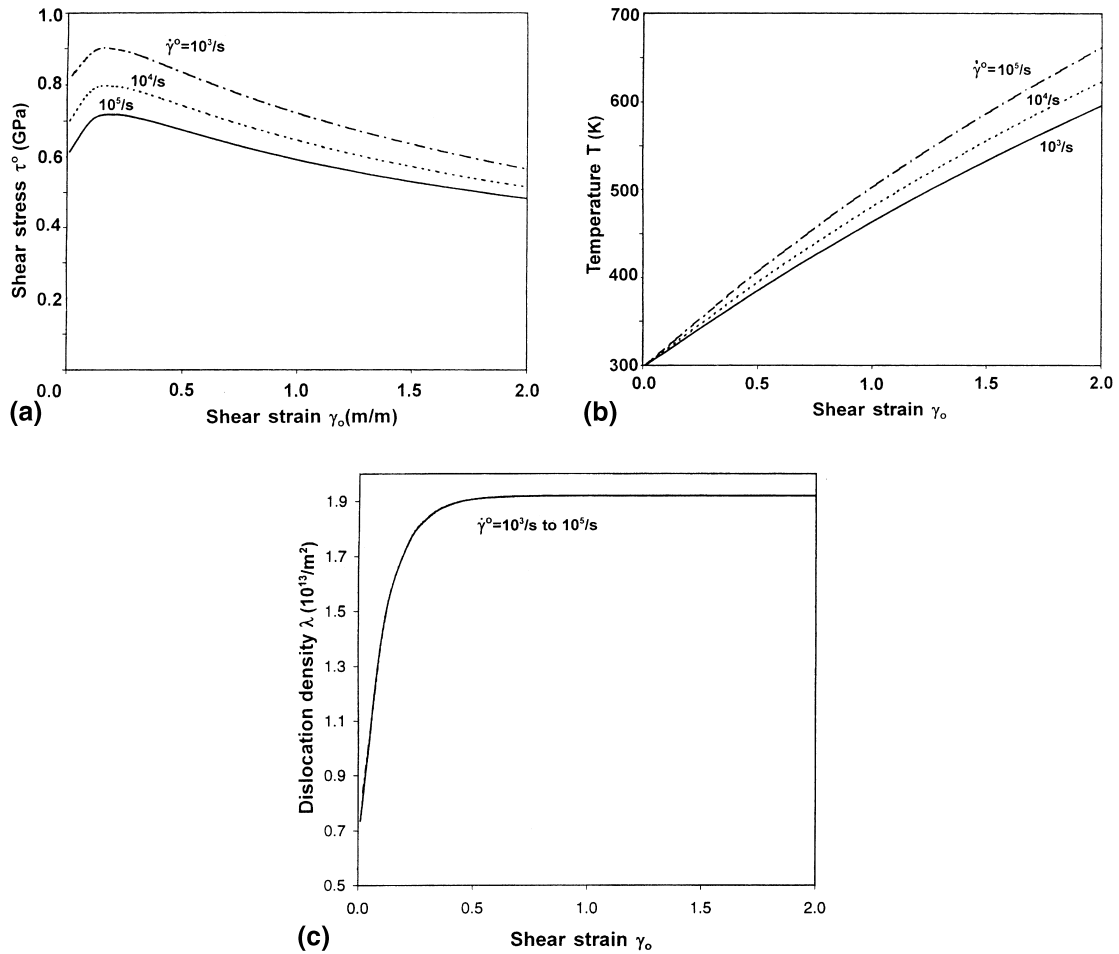


Fig. 1. Evolution of (a) shear stress, (b) temperature, and (c) dislocation density at the three different nominal strain rates.

shear stress occurs. The dislocation density λ first increases with an increase in the plastic deformation of the body and reaches a saturation value of about $1.9 \times 10^{13}/m^2$ at a plastic strain of approximately 0.6; the maximum value of λ equals $3\lambda_0$. The evolution of the dislocation density for the range of strain-rates considered herein is independent of the nominal strain-rate since K_a in Eq. (21) equals K_0 for $\dot{\gamma}^0 = 10^3, 10^4$ and $10^5/s$.

An instability will occur when the homogeneous solution satisfies the inequality (18); the minimum value of the nominal strain given by inequality (18) is denoted by γ_i^0 and is called the instability strain. For seven different values of the initial temperature T_0 , Figs. 2–4 evince the dependence of the

instability strain γ_i^0 , the corresponding shear stress τ_i^0 , and the dislocation density λ_i^0 upon the nominal strain-rate $\dot{\gamma}^0$. For a fixed value of $\dot{\gamma}^0$, the instability strain γ_i^0 increases with an increase in the initial temperature; a similar result was obtained in [17] for the structural instability strain. They used a phenomenological constitutive relation, considered the dependence of the material parameters such as the shear modulus, the specific heat and the thermal conductivity on the temperature, and the specimen had a geometric defect in it. Here only the shear modulus is taken to depend on the temperature (cf. Eq. (5)). Note that the homogeneous solution becomes unstable soon after the shear stress attains its peak value. At low initial

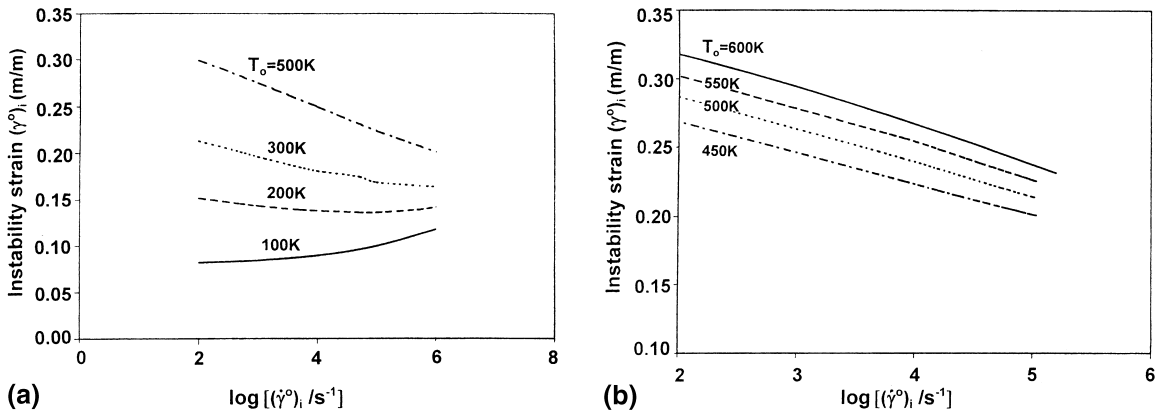


Fig. 2. For different values of the initial temperature, variations of instability strain with log of strain-rate: (a) 100–500 K and (b) 450–600 K.

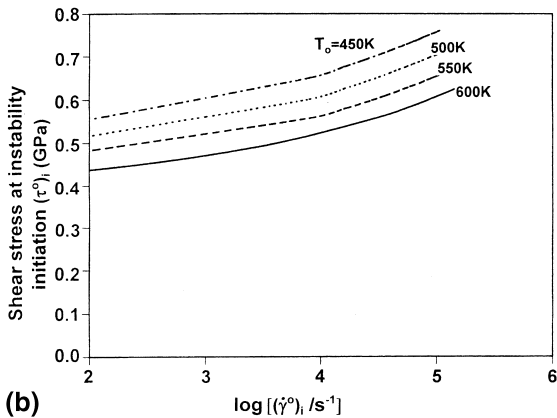
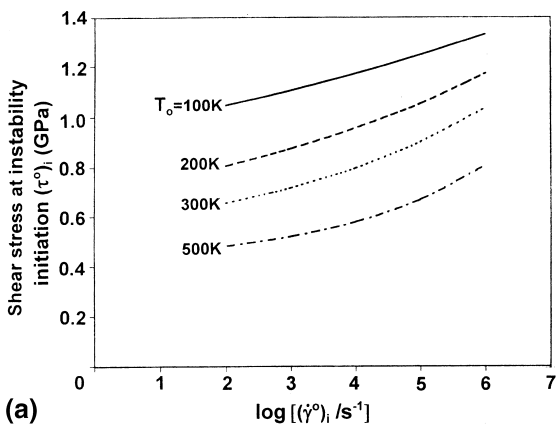


Fig. 3. For different values of the initial temperature, variations of shear stress at instability initiation with log of strain-rate: (a) 100–500 K and (b) 450–600 K.

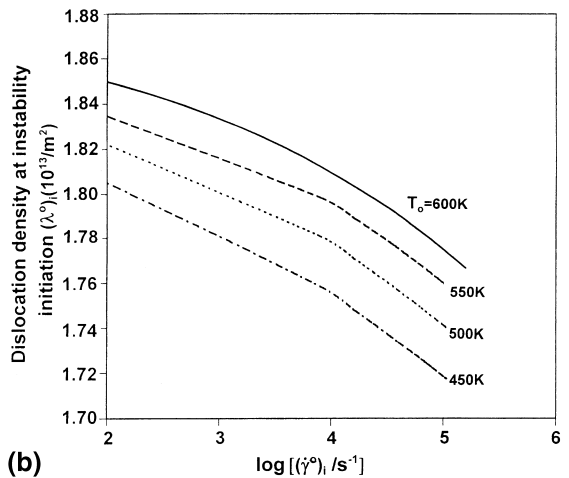
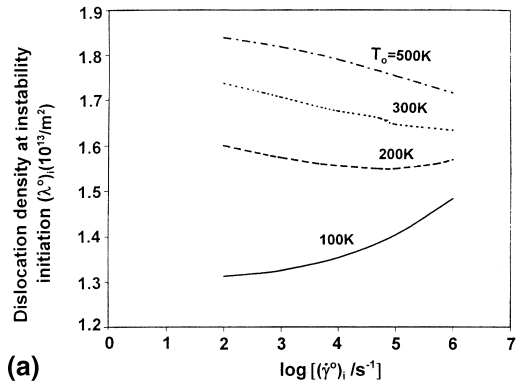


Fig. 4. For different values of the initial temperature, variations of dislocation density at instability initiation with log of strain-rate: (a) 100–500 K and (b) 450–600 K.

temperatures, the instability strain increases with an increase in the nominal strain-rate but at initial temperatures greater than or equal to 300 K, the instability strain decreases with an increase in the nominal strain-rate. For each one of the initial temperatures considered, the shear stress at the onset of material instability increases with an increase in the nominal strain-rate. The same result was obtained in [18] for four different phenomenological relations. At $T_0 = 100$ K, the dislocation density at instability sharply increases when the

nominal strain-rate is increased from 10^2 to 10^6 /s but for $T_0 = 200$ K, the change in λ_i^0 with an increase in $\dot{\gamma}^0$ is relatively very small. Also, for $T_0 \geq 300$ K, λ_i^0 decreases slowly with an increase in $\dot{\gamma}_i^0$. Note that λ_i^0 depends exponentially upon γ_i^0 , and λ_i^0 increases monotonically with γ_i^0 . Because of the rather small values of the plastic shear strain at the onset of instability, the rise in the temperature up to the initiation of instability is also quite small (about 20 K), and is essentially the same for all values of T_0 and $\dot{\gamma}^0$ considered herein.

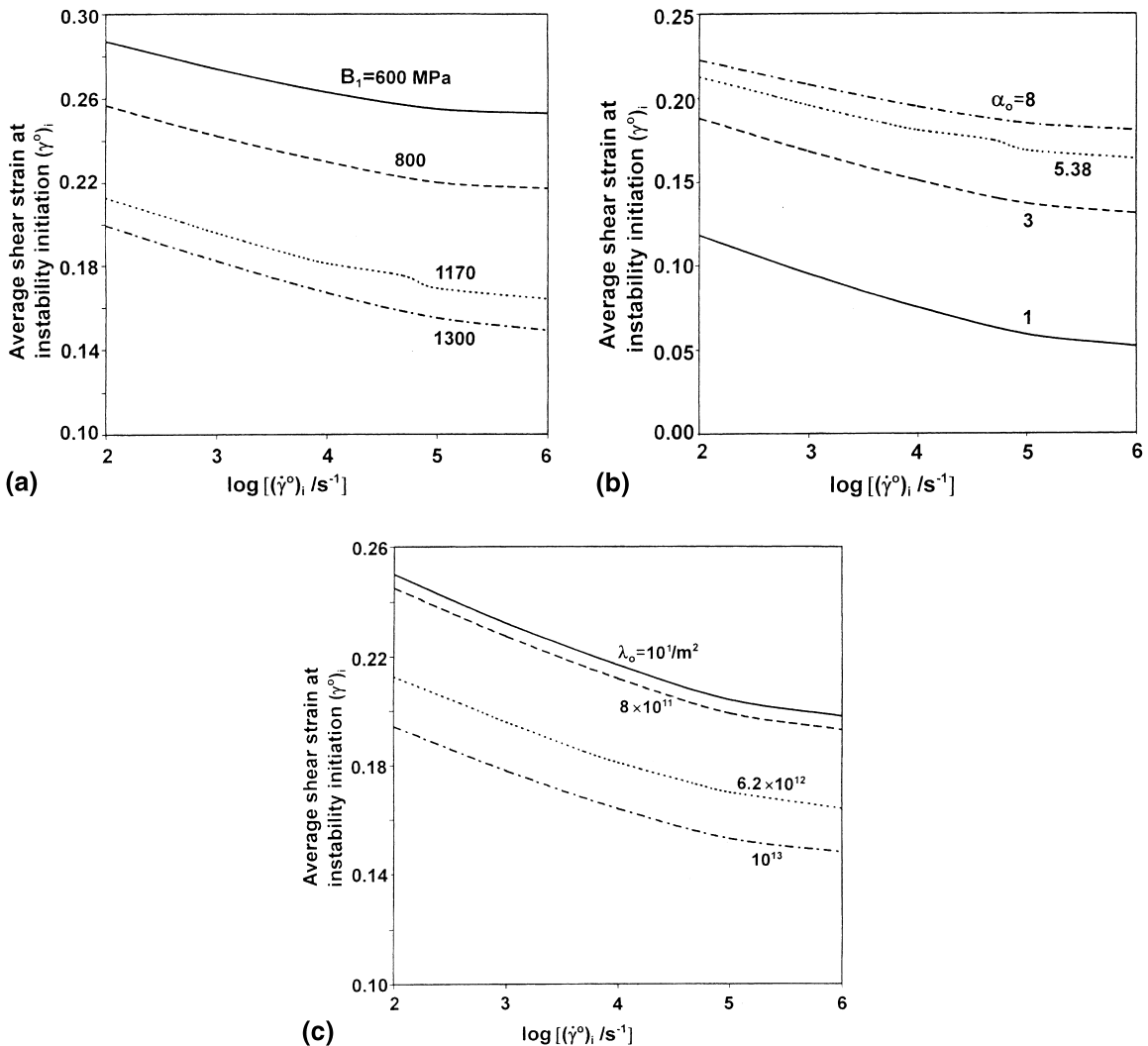


Fig. 5. Dependence of instability strain on nominal strain-rate for different values of (a) initial thermal activation parameter, (b) microstructure interaction parameter, and (c) initial dislocation density.

Figs. 5(a)–(c) exhibit the relationship between γ_i^0 and $\ln \dot{\gamma}^0$ for different values of the initial thermal activation parameter B_1 , the microstructure interaction parameter α_0 , and the initial dislocation density λ_0 . For all cases studied, the instability strain gradually decreases with an increase in the nominal strain-rate. For a fixed value of $\dot{\gamma}^0$, the instability strain decreases with an increase in the value of B_1 , a decrease in the value of α_0 , and an increase in the value of λ_0 .

5. Shear band spacing

The three roots of the spectral Eq. (11) are functions of the wave number ξ and the time t_0 or the average strain γ^0 when the homogeneous solution is perturbed. In deriving Eq. (14) and hence the instability criterion (18) the time t_0 was kept fixed. Numerical results presented above give the minimum value, γ_i^0 , of the average shear strain when the homogeneous solution if perturbed will become unstable. The dependence of the maximum growth rate, $\bar{\eta}_m$, of the perturbation on t_0 is now investigated, and roots of Eq. (11) are found. For the function f given by Eq. (20) and values of material parameters given in (24), Fig. 6 depicts,

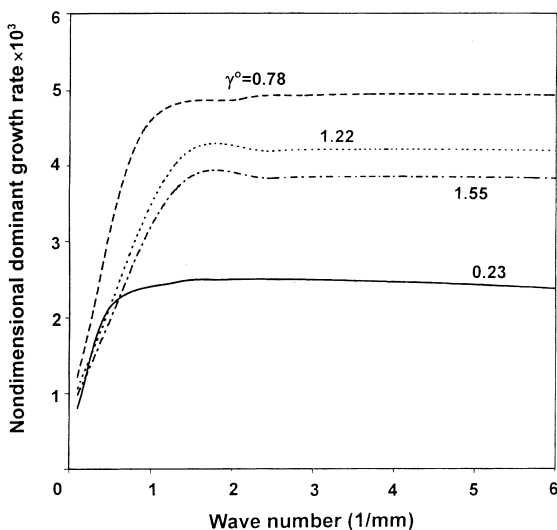


Fig. 6. Normalized dominant growth rate vs. wave number for shear strain at instants of perturbing the homogeneous solution.

for $\gamma^0 = 0.23, 0.78, 1.22$ and 1.55 , the normalized dominant growth rate of the perturbation, $\bar{\eta}_m/\dot{\gamma}_0$, as a function of the wave number ξ . The dominant growth rate corresponds to the root of Eq. (11) with the maximum real part. For each value of γ^0 , the dominant growth rate increases with an increase in the wave number, reaches a maximum value and then very slowly decreases. Henceforth, the maximum dominant growth rate at time t_0 for the perturbations is called the critical growth rate at time t_0 and the corresponding wavelength the critical wavelength. For the nominal strain-rates of $10^4/s$, Fig. 7(a) exhibits the critical growth rate as a function of the average strain when the perturbation is introduced. Also included in the figure is a plot of η_m^* as given by Eq. (16) vs. γ^0 . For a fixed γ^0 , η_m^* slightly exceeds η_m as it should. The critical growth rate is maximum at $\gamma^0 \simeq 0.5$. From the plot of the critical wavelength vs. the nominal shear strain γ^0 given in Fig. 7(b), one concludes that the critical wavelength first decreases sharply with an increase in γ^0 , reaches a minimum value and then increases very slowly. The minimum value of the critical wavelength depends strongly on the nominal strain-rate but occurs at the same value of γ^0 .

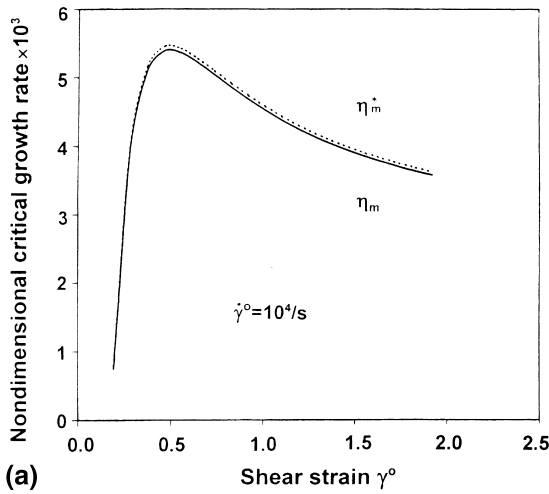
It was postulated in [5] that the wavelength of the dominant instability mode with the maximum growth rate at time t_0 determines the shear band spacing, L_s . That is,

$$L_s = 2\pi/\xi_m(t_0^m), \quad (25)$$

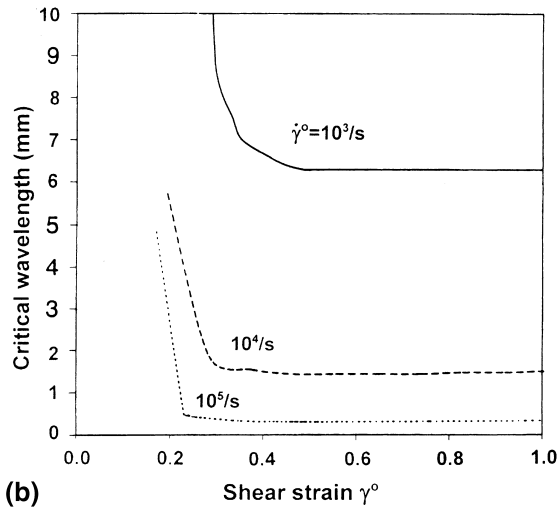
where t_0^m corresponds to the time when $\bar{\eta}_m(t_0)$ is maximum. In [4], a power-law type strain-hardening material is considered. It was found that

$$L_s = \inf_{t_0 \geq 0} (2\pi/\xi_m(t_0)) \quad (26)$$

gives essentially the same value as Eq. (25). However, it was found in [6] that the values of L_s given by Eqs. (25) and (26) differ noticeably when thermal softening of the material is modeled by an affine function of the temperature rise. Results presented below are with the definition (25) of the shear band spacing, and are for a layer of infinite thickness. Thus, the effect of boundary conditions on the shear band spacing has been neglected. This effect has been estimated in [4] to be $L_s/2H$, where $2H$ is the thickness of the layer. It is evident from



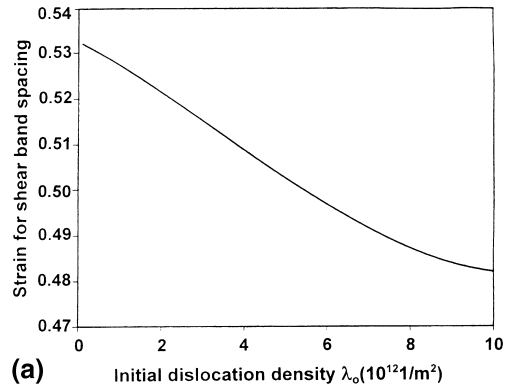
(a)



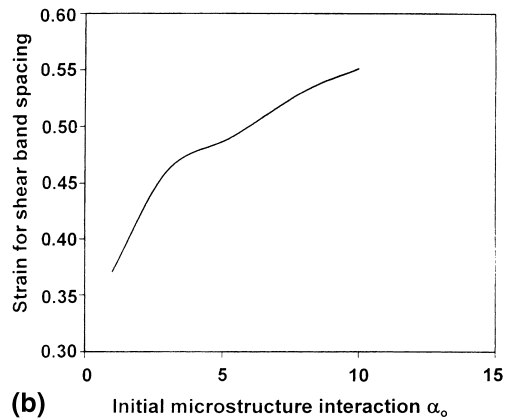
(b)

Fig. 7. Dependence on the average shear strain when the homogeneous solution is perturbed of (a) normalized critical growth rate and (b) critical wave length.

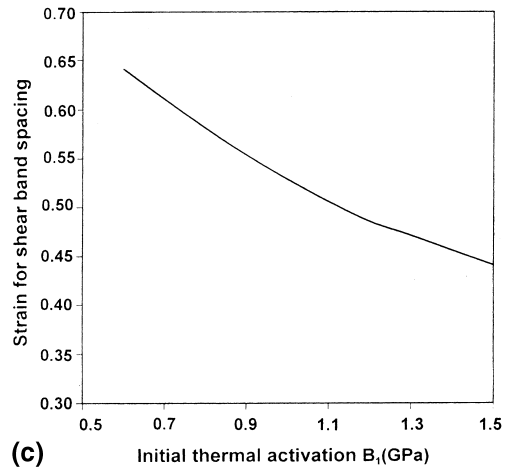
Figs. 7(a) and (b) that the critical growth rate is maximum at $\gamma^0 \simeq 0.5$ and the critical wavelength is minimum at about the same value of the nominal strain. Thus for the class of materials modeled by Eqs. (3)–(5) and (20), definitions (25) and (26) of the shear band spacing give essentially the same value of L_s . Note that the value of the shear strain corresponding to the shear band spacing is considerably higher than the values of the instability strain plotted in Fig. 2(a). Figs. 8(a)–(c) depict the



(a)



(b)



(c)

Fig. 8. Shear strain at shear band spacing vs. (a) initial dislocation density, (b) initial microstructural interaction parameter, and (c) initial thermal activation parameter.

dependence of the shear strain $\dot{\gamma}^{0s} = \dot{\gamma}^0 t^m$ corresponding to the shear band spacing upon the initial (at time zero) dislocation density λ_0 , the initial microstructure interaction parameter α_0 and the initial thermal activation parameter B_1 . The nominal strain γ^{0s} corresponding to the shear band spacing monotonically decreases with an increase in the values of B_1 and λ_0 . However, it gradually increases with an increase in the value of α_0 . The dependence of the value of γ^{0s} on λ_0 is much less predominant than that on B_1 and α_0 . Figs. 9(a)–(c) evince the variation of the shear band spacing and the nondimensionalized maximum growth rate with B_1 , λ_0 and α_0 . Out of these three microstructural parameters considered, only the initial microstructural interaction parameter has a noticeable effect on the value of the maximum growth rate of the infinitesimal perturbations. The shear band spacing decreases nearly affinely from 1.54 to 1.40 mm as λ_0 is increased from 0 to $10^{12}/\text{m}^2$, and it decreases from about 2 to 1 mm as α_0 is increased from 1 to 10. However, the shear band spacing gradually increases with an increase in the values of B_1 .

In an explosively loaded stainless steel cylinder [19], the strain-rate within a shear band was estimated to be $10^4/\text{s}$, and measured shear band spacing equalled about 1 mm. Our computed values are close to the measured value. Note that the values of material parameters listed in (24) are for a typical steel and not necessarily for the steel tested in [19].

6. Effect of dislocation drag

Eq. (4) has been modified in [9] to the form

$$\tau_1 = \frac{B_1 e^{-(\beta_1 - \beta_2 \ln \dot{\gamma})T}}{\left(1 - \frac{C\dot{\gamma}}{\beta_2 \tau_1}\right)^{\beta_2 T}}, \quad (27)$$

which accounts for the dislocation drag in their thermally activated dislocation model. The constant C in Eq. (27) describes the dislocation drag. For a BCC metal, B_1 is a constant and it is proportional to $\gamma^{1/2}$ for a FCC metal. Fig. 10(a) depicts the shear stress vs. the shear strain curves for four values of C ; values of other material param-

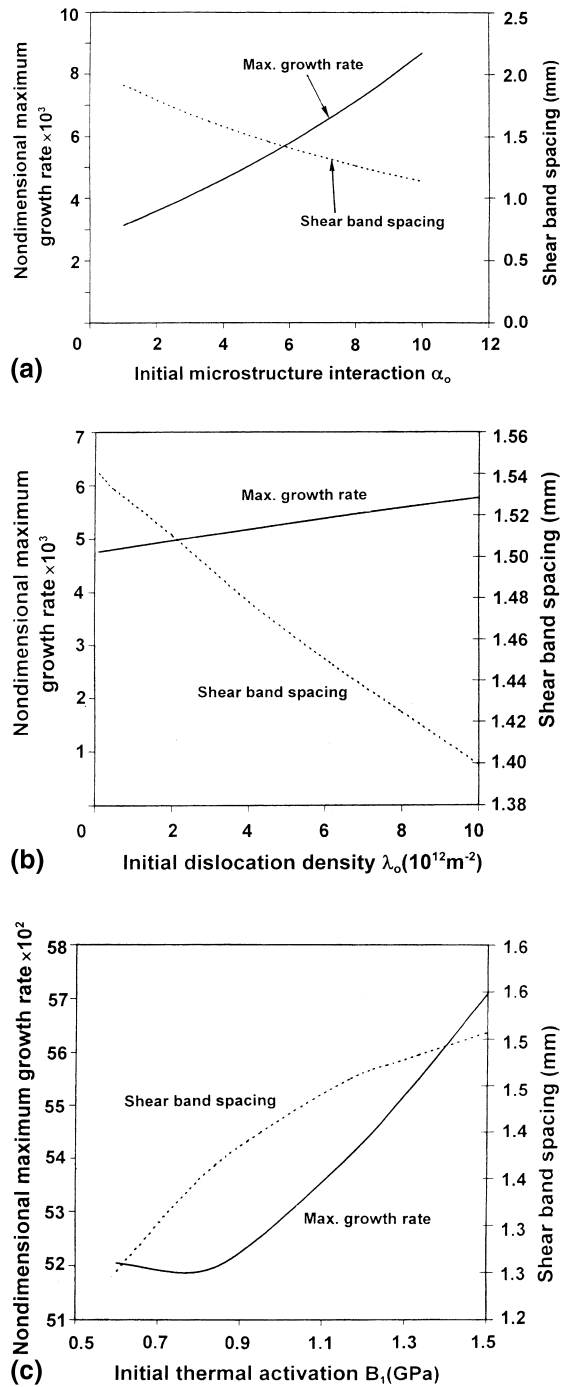


Fig. 9. Normalized maximum growth rate and shear band spacing vs. (a) initial microstructural interaction parameter, (b) initial dislocation density, and (c) initial thermal activation parameter.

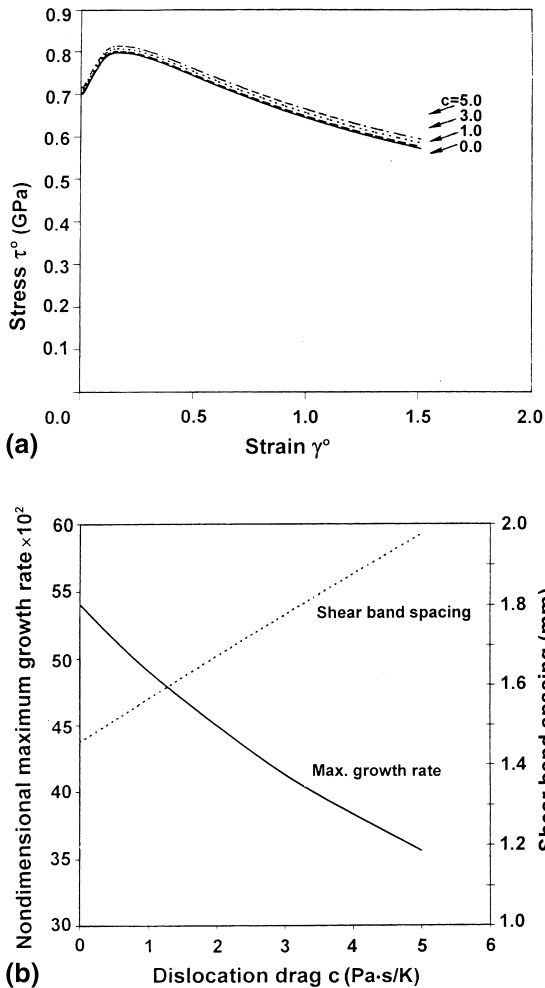


Fig. 10. Effect of the dislocation drag upon (a) shear stress vs. shear strain, and (b) shear band spacing, and the maximum growth rate.

eters are given in Eq. (24). These plots reveal that the effect of increasing C is similar to that of enhancing the nominal strain-rate. That is, for fixed values of the shear strain and the shear strain-rate, the stress required to plastically deform the body increases with an increase in the value of C . The effect of the dislocation drag on the shear band spacing and the maximum growth rate of the perturbation are exhibited in Fig. 10(b). The shear band spacing increases monotonically and the maximum growth rate decreases with an increase in the value of C from 0 to 5 Pa s/K. The computed

value of the shear band spacing is close to the experimentally observed value.

7. Conclusions

Following the work of [10,12] the shear stress has been expressed as the sum of two parts, one due to thermally activated dislocation interactions and the other described by the history of the plastic deformation through an internal variable identified as the total dislocation density. A homogeneous solution of equations governing thermomechanical deformations of the body deformed in simple shear is perturbed at time t_0 by an infinitesimal amount. The spectral equation for the growth rate at time t_0 of these perturbations is deduced, and the wavelength $\xi_m(t_0)$ corresponding to the maximum growth rate at time t_0 is found. An instability criterion that ensures the growth of the superimposed infinitesimal perturbations is derived. Also, an expression for the upper bound of the growth rate of the perturbations is obtained. The dependence of the nominal strain at the onset of material instability and of that corresponding to the shear band spacing upon various microstructural parameters are exhibited.

It is found that results computed with the proposed micromechanics model are qualitatively similar to those obtained with a phenomenological constitutive relation. The critical strain defined as the minimum average shear strain at which a homogeneous solution if perturbed becomes unstable equals that at which the shear stress attains its maximum value. The shear band spacing decreases with an increase in the value of the initial dislocation density and the initial microstructure interaction parameter, but increases with an increase in the value of the initial thermal activation parameter. The computed shear band spacing is found to be close to the measured value of 1.0 mm in a steel.

Acknowledgements

This work was supported by the ONR grant N00014-98-0300 to Virginia Polytechnic Institute

and State University with Dr. Y.D.S. Rajapakse as the program manager.

References

- [1] R.J. Clifton, Adiabatic shear in material response to ultrahigh loading rates, National Materials Advisory Board Committee, Report No. NMAB-356, 1980, pp. 129–142 (Chapter 8).
- [2] Y. Bai, Thermo-plastic instability in simple shear, *J. Mech. Phys. Solids* 30 (1982) 195–207.
- [3] L. Anand, K.H. Kim, T.G. Shawki, Onset of shear localization in viscoplastic solids, *J. Mech. Phys. Solids* 35 (1987) 427–429.
- [4] A. Molinari, Collective behavior and spacing of adiabatic shear bands, *J. Mech. Phys. Solids* 45 (1997) 1551–1575.
- [5] T.W. Wright, H. Ockendon, A scaling law for the effect of inertia on the formation of adiabatic shear bands, *Int. J. Plasticity* 12 (1996) 927–934.
- [6] R.C. Batra, L. Chen, Shear band spacing in gradient-dependent thermoviscoplastic materials, *Comput. Mech.* 23 (1999) 8–19.
- [7] L. Chen, R.C. Batra, Effect of material parameters on shear band spacing in strain-hardening gradient dependent thermoviscoplastic materials, *Int. J. Plasticity* 15 (1999) 551–574.
- [8] F.J. Zerilli, R.W. Armstrong, Dislocation mechanics based analysis of material dynamics behavior: enhanced ductility, deformation twinning, shock deformation, shear instability, dynamic recovery, *J. Phys.* 7 (1997) c3-637–642.
- [9] F.J. Zerilli, R.W. Armstrong, The effect of dislocation drag on the stress–strain behavior of FCC metals, *Acta Metall. Mater.* 40 (1992) 1803–1808.
- [10] F.J. Zerilli, R.W. Armstrong, Dislocation-mechanics-based constitutive relations for material dynamics calculations, *J. Appl. Phys.* 61 (5) (1987) 1816–1825.
- [11] J.R. Klepaczko, C.Y. Chiem, On rate sensitivity of FCC metals, instantaneous rate sensitivity and rate sensitivity of strain hardening, *J. Mech. Phys. Solids* 34 (1986) 29.
- [12] J.R. Klepaczko, A general approach to rate sensitivity and constitutive modeling of FCC and BCC metals, in: A.A. Balkema (Ed.), *Impact: Effects of Fast Transient Loadings*, Rotterdam, 1988, p. 3.
- [13] J.R. Klepaczko, Modeling of structure evolution at medium and high strain rates, FCC and BCC metals, in: *Constitutive Relations and Their Physical Basis*, Riso Natl. Lab., Roskilde, Denmark, 1997, p. 387.
- [14] J.R. Klepaczko, B. Rezaig, A numerical study of adiabatic shear banding in mild steel by dislocation mechanics based constitutive relations, *Mech. Mater.* 24 (1996) 125–139.
- [15] R.C. Batra, The initiation and growth of, and the interaction among adiabatic shear bands in simple and dipolar materials, *Int. J. Plasticity* 3 (1987) 75–89.
- [16] R.C. Batra, C.H. Kim, Analysis of shear bands in twelve materials, *Int. J. Plasticity* 8 (1992) 425–452.
- [17] C.H. Kim, R.C. Batra, Effect of initial temperature on the initiation and growth of shear bands in a plain carbon steel, *Int. J. Nonlinear Mech.* 27 (1992) 279–291.
- [18] R.C. Batra, L. Chen, Effect of viscoplastic relations on the instability strain, shear band initiation strain, the strain corresponding to the minimum shear band spacing, and the band width in a thermoviscoplastic material, *Int. J. Plasticity* (in press).
- [19] V.F. Nesterenko, M.A. Meyers, T.W. Wright, Collective behavior of shear bands, in: L.E. Murr, K.P. Staudhammer, M.A. Meyers (Eds.), *Metallurgical and Materials Applications of Shock-Wave and High-Strain-Rate Phenomena*, Elsevier, Amsterdam, 1995, pp. 397–404.